



ARTICLE

Compulsive alcohol consumption is regulated by dorsal striatum fast-spiking interneurons

Michael S. Patton¹, Morgan Heckman¹, Cecelia Kim¹, Chaoqi Mu¹ and Brian N. Mathur¹

Compulsive alcohol consumption is a core, treatment-resistant feature of alcohol use disorder. The dorsomedial and dorsolateral striatum support goal-directed and habitual action strategies, respectively. How ethanol targets dorsolateral striatum to drive compulsive consumption is poorly understood. Parvalbumin-expressing striatal fast-spiking interneurons comprise ~1% of the total neuronal striatal population, are enriched dorsolaterally and are functionally modulated by ethanol. To test whether fast-spiking interneurons are necessary for the development of compulsive ethanol consumption, we selectively ablated these neurons in adult male and female C57BL/6J mice undergoing a voluntary chronic intermittent ethanol consumption paradigm followed by a compulsive ethanol drinking assay. Fast-spiking interneuron ablation curtailed the development of organized ethanol lick sequence behavior, reduced ethanol consumption, and abrogated compulsive consumption of ethanol with the added bitterant quinine. In contrast, fast-spiking interneuron ablation did not affect any index of water or sucrose consumption. These data causally implicate the minority striatal fast-spiking interneuron population as a key component of compulsive ethanol consumption.

Neuropsychopharmacology (2021) 46:351–359; <https://doi.org/10.1038/s41386-020-0766-0>

INTRODUCTION

Repeated exposure to drugs of abuse, like alcohol, facilitates habit learning and thwarts efforts to abstain from further consumption [1, 2]. Chronic alcohol users increase habitual responding on stimulus-response task and this correlates with the duration of alcohol dependence [3, 4]. In rodents, chronic ethanol exposure promotes habitual ethanol consumption [5, 6] and accelerates habitual responding for sucrose reward [7]. Collectively, this suggests that chronic ethanol exposure targets neuronal substrates governing habit formation. Determining these substrates is the first step toward devising strategies toward treating compulsive alcohol drinking, which is notoriously treatment resistant [8–12].

Habitual behavior requires a dynamic interaction between the cortex and basal ganglia [13–17]. Lesion studies demonstrate the necessity of the dorsolateral striatum, which is innervated by sensorimotor cortices, in the acquisition and expression of habitual behavior [18–21]. The dorsolateral striatum is characterized by an enrichment of the parvalbumin (PV) expressing fast-spiking interneurons (FSIs) that provide powerful inhibitory control over striatal medium spiny projection neurons [22–27]. FSIs are implicated in habitual responding for a sucrose reward [28]. Whether FSIs are a key ethanol target giving rise to compulsive ethanol consumption is not known.

Ethanol alters FSI intrinsic excitability [29] and disrupts FSI synaptic transmission onto medium spiny projection neurons [30]. This supports the possibility that ethanol targets FSIs to promote compulsive consumption. Therefore, in the following study, we selectively ablated dorsal striatal FSIs in both male and female C57BL/6J mice undergoing a voluntary chronic intermittent ethanol consumption paradigm, drinking-in-the-dark (DID). We analyzed lick sequence behavior across the drinking paradigm to determine if striatal FSIs regulate lick behavior seen in compulsive

drinking rats [31]. We found that FSI ablation reduced ethanol consumption and disorganized ethanol lick sequence behavior. Additionally, when ethanol is adulterated with the bitterant quinine, FSI ablation attenuated ethanol consumption. Collectively these results provide evidence for a causal role of dorsal striatum FSIs in compulsive ethanol consumption.

METHODS

All experiments were performed in accordance with NIH guidelines and were approved by the Institutional Animal Care and Use Committee of the University of Maryland Baltimore and the National Institute on Alcohol Abuse and Alcoholism. Mice were housed with littermates (2–5 per cage) under a reverse 12-h light/dark cycle (lights off at 0900 h, on at 2100 h) with *ad libitum* access to food and water.

FSI ablation

To selectively ablate PV-containing FSIs in the dorsal striatum, ≥2-month old PV-*cre* transgenic mice on a C57BL/6J background [32, 33] were injected bilaterally with AAV5-flex-taCasp3-TEVP (UNC, Chapel Hill Vector Core) or AAV5-dio-EYFP (Addgene) at a volume of 500 nl/side and a rate of 20 nl/min at the following coordinates relative to bregma: anterior-posterior +0.6 mm; medial-lateral ±2.25 mm; dorsal-ventral –3.4 mm.

Mice were initially anesthetized with 4% vaporized isoflurane (VetEquip) and maintained at 1–2.5% isoflurane for the duration of the surgery based on a toe-pinch response. A topical analgesic (2% lidocaine) was applied to the incision site following surgery. For additional pain management, mice received a daily injection of carprofen (5 mg/kg, i.p.) three days following surgery. Mice received a three-week recovery period before behavioral testing.

¹Department of Pharmacology, University of Maryland School of Medicine, Baltimore, MD 21201, USA
Correspondence: Brian N. Mathur (bmathur@som.umaryland.edu)

Received: 23 April 2020 Revised: 22 June 2020 Accepted: 8 July 2020
Published online: 14 July 2020

Drinking-in-the-dark (DID)

The DID protocol was adapted from Rhodes et al. [34]. Mice (5 males, 5 females per group) were randomly assigned to the water, sucrose, or ethanol drinking groups. Two hours into the dark cycle (1100) mice were placed into modified home cages (18×18×23 cm) with *ad libitum* access to food that was weighed at the end of each week. In order to achieve a clean lickometer signal, we elevated the drinking spout to disallow climbing and paw grabbing, which created false signals on the lickometer. Since mice did not drink 20% ethanol from this spout height spontaneously but would instead learn to drink from an elevated sipper providing a sucrose solution, we added a four-day sucrose fading session to train our mice to drink from the elevated sipper prior to the four-week DID procedure (i.e., week 0). During the four-week DID procedure, mice were given two hours of access to the drinking bottle in the first three days, and on day four, mice were given four hours of access. Following four days of drinking, mice underwent three days of forced abstinence. On week 4, blood samples were collected from tail nicks immediately following a 2-h session to determine the blood ethanol concentration. Blood serum values were measured spectrophotometrically using an enzymatic assay (Sigma MAK076). On weeks 0 and 4, mice were given a two-bottle choice test of water and ethanol (2-h duration) to determine drinking preference. On days two through four of week 5, the bitterant quinine (0.3 mM) was added to the bottles to assess compulsive drinking.

Lickometer

A grated steel platform was placed on the floor of the chamber below the metal sipper of the drinking bottle and was connected to the ground of an analog-to-digital (AD) converter (Digidata, Molecular Devices). The input signal was connected to the metal sipper that created a circuit that closed when the mouse licked the sipper while standing on the steel platform. Lick events were recorded using Clampex software (Molecular Devices). Data were analyzed offline with Matlab (Mathworks R2018a). Events of 1–2 licks were defined as unorganized licks, while events of ≥3 licks, each lick occurring within 2 s or less, were classified as organized drinking bouts [35].

Immunohistochemistry and ablation quantification

Mice (4 males, 3 females per group) were anesthetized with isoflurane and then intracardially perfused with saline followed by ice-cold paraformaldehyde (4%). Fixed brains were extracted and 100 μm sections were collected using a vibratome (Leica). Slices were incubated in a mouse anti-PV antibody (1:1,000; clone PARV-19, Sigma-Aldrich) overnight at 23 °C. The following day, slices were washed with a solution of phosphate-buffered saline with Triton-X100 (0.2%) and incubated in Cy3 conjugated secondary antibody for four hours at 23 °C (1:2,000; Jackson ImmunoResearch). Fluorescent images were visualized on a Nikon Eclipse Ti2 fluorescent microscope and captured with a Nikon DS-Qi2 camera. Cell counts were blindly collected from a region of interest encompassing the dorsolateral striatum. Automated cell counts were performed with Nikon Instruments Elements Advanced Research software (5.11.01). In brief, fluorescent signal was restricted to a three-point circle threshold, and objects were excluded based on object circularity and diameter.

Acute slice preparation

Mice (3 males, 2 females per group) were deeply anesthetized with isoflurane then perfused with a carbogen-bubbled N-Methyl-D-Glutamine (NMDG) artificial cerebral spinal fluid (aCSF) solution (92 mM NMDG, 2.5 mM KCL, 1.25 mM NaH₂PO₄, 30 mM NaHCO₃, 20 mM HEPES, 25 mM glucose, 2 mM thiourea, 5 mM Na-ascorbate, 3 mM NA-pyruvate, 0.5 mM CaCl₂, and 10 mM MgCl₂) before decapitation and brain removal. 250 μm coronal sections were collected in ice-cold NMDG aCSF. Sections were incubated at 32 °C

for 12 minutes and then transferred to HEPES holding solution (92 mM NaCl, 2.5 mM KCL, 1.25, 1.25 mM NaH₂PO₄, 30 mM NaHCO₃, 20 mM HEPES, 25 mM glucose, 2 mM thiourea, 5 mM Na-ascorbate, 3 mM NA-pyruvate, 2 mM CaCl₂, and 2 mM MgCl₂) and stored at room temperature until recording.

Whole-cell voltage-clamp electrophysiology

Slices were hemisected, placed into a recording chamber, and perfused with temperature-controlled aCSF (29–31 °C) containing 50 μM DL-AP5 and 5 μM NBQX. Dorsolateral striatum medium spiny neurons were visualized using infrared differential interference contrast light microscopy and Q-capture camera and associated Pro 7 software. Striatal medium spiny projection neurons (MSNs) were voltage clamped at –60 mV using a MultiClamp 700B Amplifier (Molecular Devices). Spontaneous inhibitory postsynaptic current (IPSC) events were recorded using a borosilicate glass pipette (3–5 MO resistance) filled with CsCl-based internal solution (150 mM CsCl, 10 mM HEPES, 2 mM MgCl₂, 0.3 mM Na-GTP, 5 mM QX-314, 3 mM Mg-ATP, and 0.2 mM BAPTA). Signals were filtered at 2 kHz, digitized at 10 kHz and acquired using Clampex 10.4.1.4 software (Molecular Devices). Data were analyzed offline using Mini Analysis Program (Synaptosoft).

Behavior in the open field

Mice (5 males, 5 females per group) were habituated to a plexiglass open-field arena (30×30×25 cm) affixed with a ceiling camera to register mouse locomotor behavior via Ethovision (Noldus). The following day, mice received an intraperitoneal (i.p.) injection of ethanol (2 mg/kg) that was previously shown to produce blood ethanol concentrations (BECs) comparable to that achieved by DID [34]. 30 minutes after injection, mice were placed in the open-field arena and locomotor behavior was recorded for 15 minutes. The following day an additional open-field trial was conducted to collect sober locomotor activity. All treatment groups were counterbalanced for ethanol and baseline trials.

Statistical analysis

All statistical analyses were performed in GraphPad Prism 8.0. Data are represented as mean ± SEM. Fluid consumption and the number of drinking bouts are derived from the weekly averages collected from the 2 h drinking sessions. Bout length, bout length distribution, and coefficient of variation are derived from bouts expressed throughout the 4-week DID paradigm. Comparisons between two groups were analyzed with a Student's *t* test while comparisons of three or more groups were analyzed with two-way ANOVA. Multiple comparisons were corrected with Sidak's test or Dunnett's test when comparing multiple time points to a single baseline. Effect sizes are reported by partial eta squared. Horizontal brackets indicate statistical significance within a treatment group, while vertical brackets indicate statistical significance between treatment groups. Simple linear regression was performed for correlation analysis and all *p* < 0.05 designations indicate a slope that is significantly non-zero. For all data, *N* is defined as an individual animal. For patch clamp data, *N* consists of an average recording from two to three cells for each animal.

RESULTS

FSI ablation was achieved using injections of control fluorophore (control)- or genetically engineered caspase3 (taCasp3)- expressing viruses into the dorsal striatum (Fig. 1). Viral-mediated FSI ablation resulted in a significant decrease in the number of PV-immunoreactive cells in the dorsolateral striatum (control = 186.4 ± 29.4 cells, taCasp3 = 34.43 ± 8.0 cells; *t*₁₂ = 4.987, *p* < 0.005, *η*² = 0.67, Student's *t* test, Fig. 1a–c). FSI ablation was further characterized by recording spontaneous IPSC events from MSNs in the dorsolateral striatum using whole-cell voltage clamp electrophysiology. FSI ablation significantly

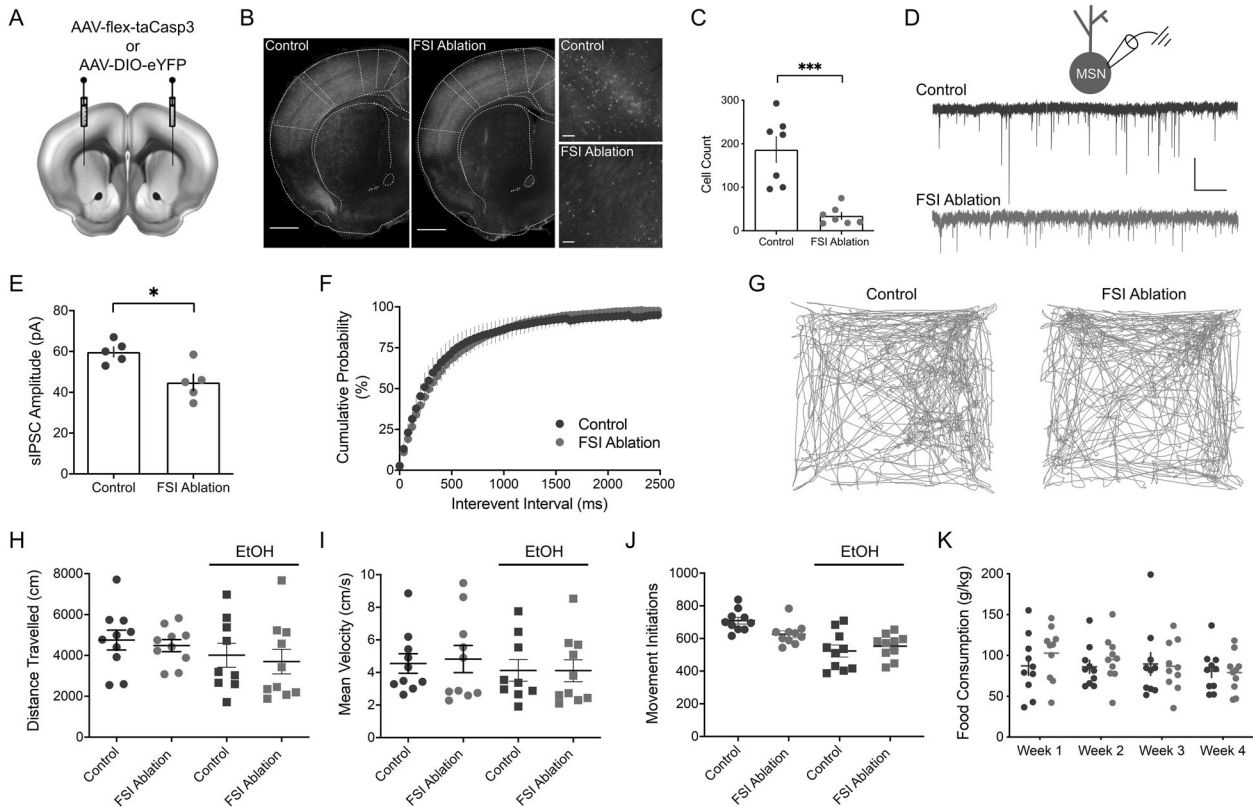


Fig. 1 Ablation of striatal fast-spiking interneurons (FSIs). **a** A schematic depicting bilateral injection sites of genetically engineered caspase 3 (taCasp3)-expressing virus for dorsal striatal FSI ablations. **b** Immunostain for parvalbumin from control (left) and taCasp3-ablated (middle) animals. Scale bar 1000 μm . 20x magnification of parvalbumin expression from control (top right) and taCasp3 ablated (bottom right) animals. Scale bar 100 μm . **c** taCasp3-mediated FSI ablation significantly reduced the number of parvalbumin-positive neurons in the dorsal striatum ($N = 7$ animals). **d** A schematic of whole-cell voltage-clamp recording of a medium spiny neuron (MSN) (top). Representative traces of spontaneous inhibitory postsynaptic current (sIPSC) events recorded from MSNs from control (dark gray) and FSI-ablated (blue) animals (bottom). Scale bars: vertical, 50 pA; horizontal, 5 s. **e** taCasp3-mediated FSI ablation reduced sIPSC event amplitude ($N = 5$ animals). **f** A cumulative frequency distribution of sIPSC event frequency showing that frequency was not affected by FSI ablation ($N = 5$ animals). **g** Representative ambulatory traces from control and FSI-ablated animals exploring an open-field arena. FSI ablation does not affect total distance traveled (**h**), mean velocity (**i**), or the number of movement initiations (**j**) in either a sober state or following acute injection of ethanol (EtOH, 2 mg/kg i.p.). **k** FSI ablation does not affect food consumption in EtOH drinking mice. * $p < 0.05$, *** $p < 0.005$. Data represented as mean \pm SEM.

decreased the amplitude of sIPSC events (control = 59.78 ± 2.41 pA, FSI ablation = 44.83 ± 3.9 pA; $t_{(8)} = 3.217$, $p < 0.05$, $\eta^2 = 0.56$, Student's t test, Fig. 1d, e) but had no effect on sIPSC event frequency ($t_{(8)} = 0.13$, $p = 0.90$, Student's t test, Fig. 1f).

To determine if FSI ablation affected gross motor function under normal or inebriated conditions, we analyzed locomotor behavior in an open field arena. We found no main effect of FSI ablation on total distance traveled under baseline conditions or following an acute injection of ethanol (2 mg/kg, i.p.) ($F_{(1,35)} = 0.342$, $p = 0.56$, two-way ANOVA, Fig. 1g, h). No main effect of FSI ablation was observed for mean velocity in the control condition or following acute injection of ethanol (2 mg/kg, i.p.) ($F_{(1,35)} = 0.032$, $p = 0.86$, two-way ANOVA, Fig. 1i). Additionally, we found no main effect of FSI ablation on the number of movement initiations in the control condition or following acute ethanol administration ($F_{(1,36)} = 1.03$, $p = 0.32$, two-way ANOVA, Fig. 1j).

To examine whether food consummatory behavior was disrupted by FSI ablation, which may indirectly affect ethanol consumption through differences in daily caloric intake, we measured weekly food pellet consumption ingested during DID. We found no main effect of FSI ablation on food consumption in water drinking animals ($F_{(1,18)} = 0.16$, $p = 0.70$; two-way ANOVA) or in ethanol drinking animals ($F_{(1,36)} = 0.26$, $p = 0.61$, two-way ANOVA, Fig. 1k). Additionally, we found no effect of time on consumption in either water ($F_{(3,46)} = 2.7$, $p = 0.065$, two-way

ANOVA) or ethanol drinking animals ($F_{(2,41)} = 1.31$, $p = 0.28$, two-way ANOVA).

During the four-week DID paradigm fluid consumption was tracked using a custom lickometer, and the data for the 2-h sessions were analyzed as they represented the large majority of all drinking sessions (Fig. 2a, b). We found that licks positively correlated with ethanol consumption (g/kg) for both control ($R^2 = 0.30$, $p < 0.001$) and FSI ablated animals ($R^2 = 0.34$, $p < 0.001$). We found no main effect of FSI ablation on water consumption ($F_{(1,18)} = 0.384$, $p = 0.543$, two-way ANOVA, Fig. 2c) or sucrose consumption ($F_{(1,18)} = 0.0282$, $p = 0.8684$, two-way ANOVA, Fig. 2d). However, we found a main effect of FSI ablation on ethanol consumption that was significantly different by week 4 (control = 71.25 ± 6.52 licks, FSI ablation 49.28 ± 3.76 licks, $F_{(1,18)} = 5.73$, $p < 0.05$, $\eta^2 = 0.14$, two-way ANOVA; Sidak's multiple comparisons test, Fig. 2e).

To determine if this reduction in licks in the ablated group was driven by changes in ethanol preference, we subjected mice to a two-bottle choice task at the beginning and end of the DID procedure. Both control (baseline = 51.04 ± 2.70 %, post-DID = 72.27 ± 4.00 %, $t_{(18)} = 5.44$, $p < 0.001$, $\eta^2 = 0.60$, Student's t test) and FSI-ablated animals exhibited a significant preference for ethanol over water consumption (baseline = 51.43 ± 3.56 %, post-DID = 68.29 ± 3.98 %; $t_{(18)} = 3.197$, $p < 0.01$, $\eta^2 = 0.38$, Student's t test, Fig. 2f).

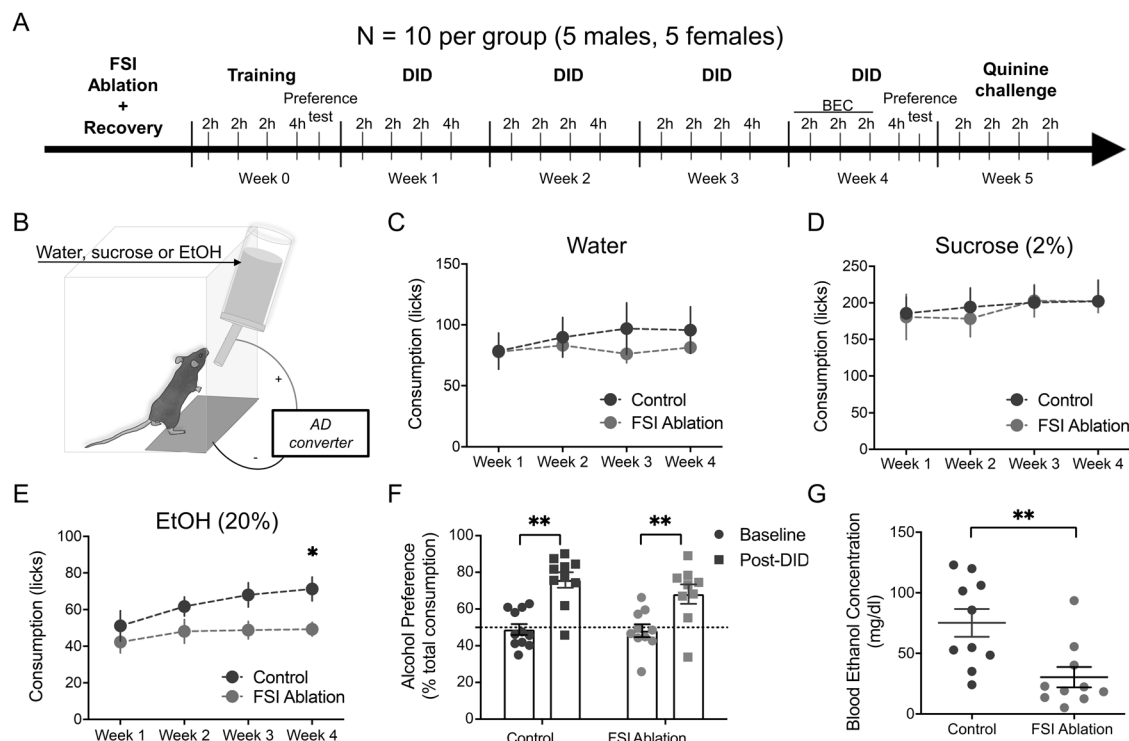


Fig. 2 Striatal FSI ablation reduced voluntary ethanol consumption. **a** Experimental timeline of FSI ablation, drinking-in-the-dark (DID), EtOH preference tests, and quinine challenge. **b** Schematic of the DID lickometer apparatus including the analog-to-digital (AD) converter. **c–e** Average weekly fluid consumption (number of licks) from control (black) and FSI ablated animals (blue) collected from two hour (2 h) DID sessions across the four-week drinking paradigm. FSI ablation did not affect water consumption (**c**) or sucrose consumption (**d**), but reduced alcohol consumption in week 4 only (**e**). **f** Both control and FSI-ablated animals exhibited an EtOH preference following the four-weeks of EtOH consumption. **g** Blood ethanol concentration from animals during week 4 of DID were lower in FSI-ablated animals. * $p < 0.05$, ** $p < 0.01$. Data represented in mean \pm SEM.

To assess BEC, blood was collected during week 4 of the DID paradigm. Control animals exhibited higher BECs compared to FSI ablated littermates (control = 75.2 ± 11.5 mg/dl, FSI ablation = 30.35 ± 8.40 mg/dl, $t_{(18)} = 3.15$, $p < 0.01$, $\eta^2 = 0.36$ Student's *t* test, Fig. 2g). The significant reduction in BEC in the face of a modest reduction in total ethanol consumption during week 4 spurred us to analyze which group drank more at end the of the session, when blood was collected, relative to total consumption on the day of blood collection. We found that control animals exhibited relatively more licks in the last 30 min than FSI ablated animals (control = 34.47 ± 3.93 %, FSI ablated = 20.62 ± 3.82 %, $t_{(16)} = 2.528$, $p < 0.05$, $\eta^2 = 0.28$ Student's *t* test).

Since the dorsal striatum is implicated in motor sequence learning [36–39], and organized lick bouts are implicated in compulsive ethanol consumption in rats [31], we examined whether striatal FSIs influence ethanol lick sequence behavior (Fig. 3). We found no main effect of FSI ablation on the number of water licking bouts ($F_{(1,18)} = 0.16$, $p = 0.69$, two-way ANOVA, Fig. 3a, d), or sucrose licking bouts ($F_{(1,18)} = 0.013$, $p = 0.91$, two-way ANOVA, Fig. 3b, e), but found that FSI ablation reduced the number of ethanol licking bouts (control = 15.28 ± 1.01 licks, FSI ablation = 9.55 ± 0.27 licks, $F_{(1,18)} = 11.75$, $p < 0.01$, $\eta^2 = 0.26$, two-way ANOVA, Fig. 3c, f). Additionally, we found a main effect of time in the ethanol drinking animals, where the control mice exhibited an increase in the number of ethanol drinking bouts by week 3, which was not observed in FSI-ablated animals (week 1 control: 11.02 ± 1.9 , week 4 control = 16.63 ± 2.01 , $F_{(3,54)} = 3.12$, $p < 0.05$, $\eta^2 = 0.06$, Dunnett's multiple comparisons test, Fig. 3f). However, we found no main effect of FSI ablation on unorganized licks from mice consuming water ($F_{(1,71)} = 0.04$, $p = 0.84$, two-way ANOVA, Fig. 3g), sucrose ($F_{(1,71)} = 0.02$, $p = 0.89$, two-way ANOVA, Fig. 3h) or ethanol ($F_{(1,71)} = 2.45$, $p = 0.12$, two-way ANOVA, Fig. 3i).

We next examined if FSI ablation altered bout licking microstructure (Fig. 4). We found that FSI ablation had no effect on the average bout length of water drinking animals ($t_{(18)} = 0.06$, $p = 0.95$, Student's *t* test, Fig. 4a, d) or sucrose drinking animals ($t_{(18)} = 1.09$, $p = 0.29$, Student's *t* test, Fig. 4b, e). However, FSI ablation increased the average bout length in ethanol drinking animals (control = 4.40 ± 0.20 licks, FSI ablation = 5.53 ± 0.41 licks, $t_{(18)} = 2.49$, $p < 0.05$, $\eta^2 = 0.26$, Student's *t* test, Fig. 4c, f). We then performed a frequency distribution analysis of bout lengths to determine the source of this mean difference. We found no effect of FSI ablation on bout length distribution from water ($F_{(1,72)} = 0.038$, $p = 0.85$, two-way ANOVA, Fig. 4g) or sucrose drinking animals ($F_{(1,72)} = 0.01$, $p = 0.99$, two-way ANOVA, Fig. 4h). However, there was a significant size \times ablation interaction in the ethanol drinking condition ($F_{(3,72)} = 10.17$, $p < 0.001$, $\eta^2 = 0.11$) where FSI-ablated animals exhibited a significant decrease in the proportion of small ethanol bouts (three to four licks per bout) in FSI-ablated animals (control = 50.45 ± 2.53 %, FSI ablation = 33.75 ± 4.17 %) and an increase in the proportion of large ethanol bouts (nine or more licks per bout) (control = 7.61 ± 1.85 %, FSI ablation = 18.64 ± 4.12 %, Sidak's multiple comparisons test, Fig. 4i). We noticed that FSI ablated animals exhibited a wider distribution of bout lengths from our frequency distribution. We therefore calculated the coefficient of variance for the bout length exhibited by each animal, and compared mean-variance across treatment group for each drinking condition. We found that FSI ablation had no effect on water ($t_{(18)} = 0.95$, $p = 0.35$, Student's *t* test, Fig. 4j) or sucrose bout length variance ($t_{(18)} = 0.36$, $p = 0.72$, Fig. 4k). However, consistent with our frequency distribution data, we found that ethanol-drinking FSI-ablated animals exhibited more bout length variance compared to controls (control 40.26 ± 2.61 %, FSI ablation 55.66 ± 5.34 %, $t_{(18)} = 2.59$, $p < 0.05$, $\eta^2 = 0.27$, Student's *t* test, Fig. 4l).

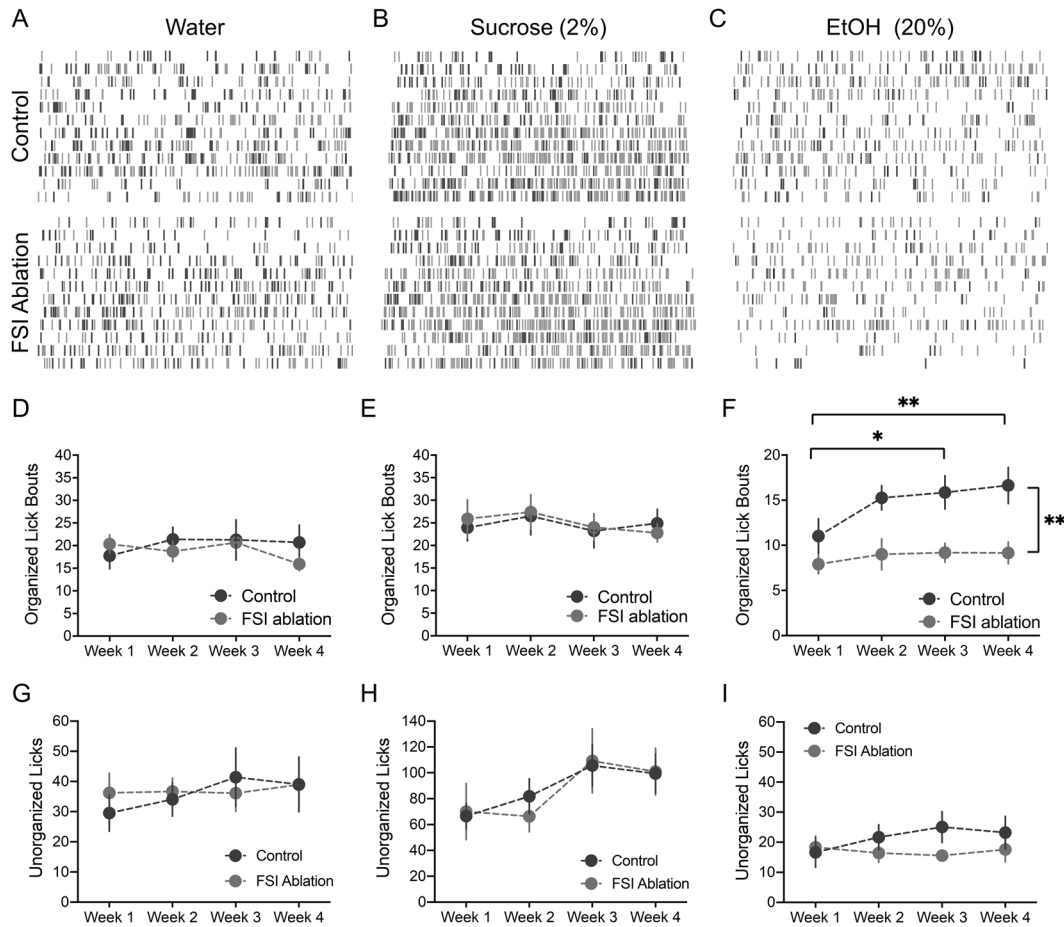


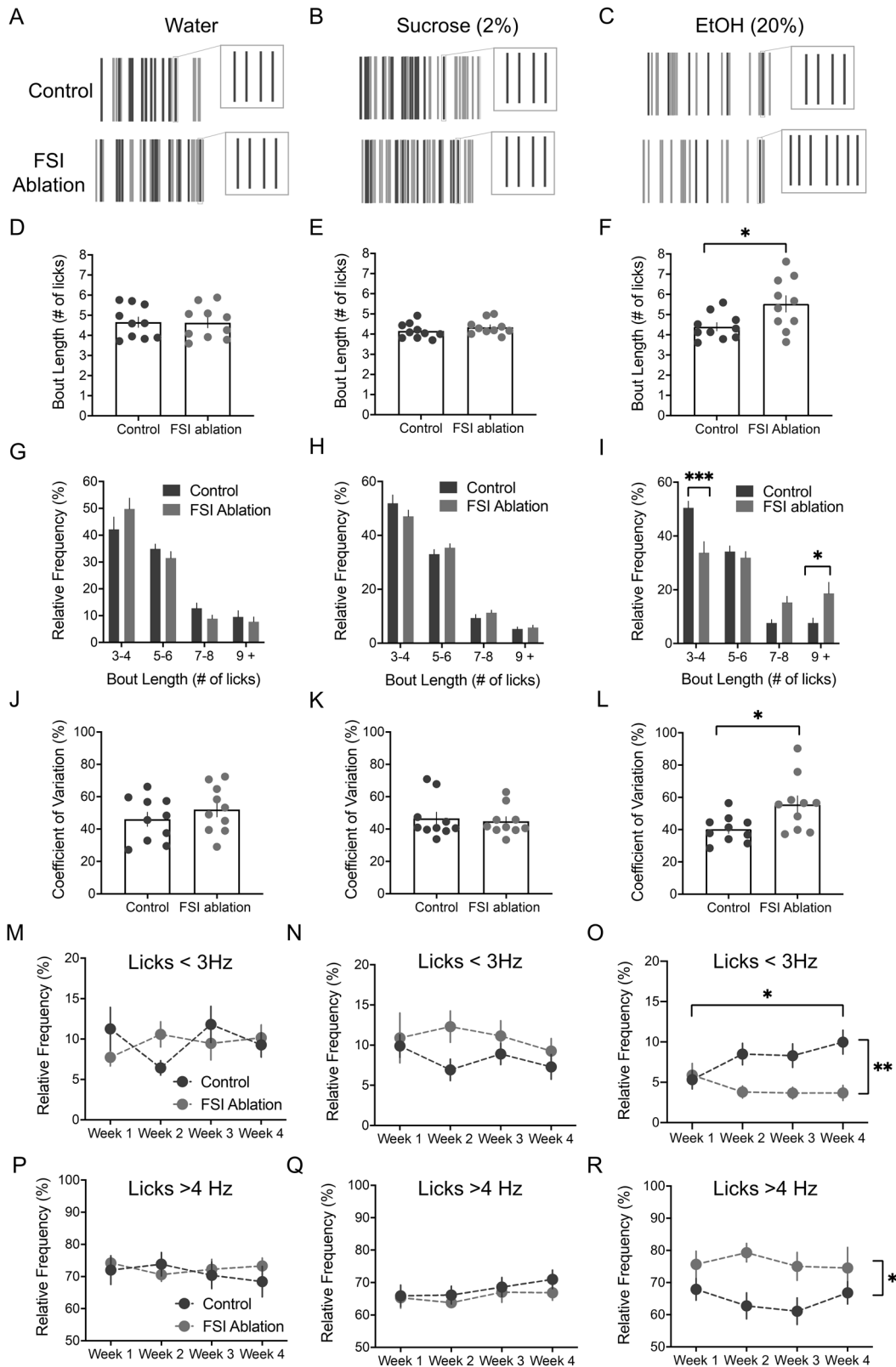
Fig. 3 Striatal FSI ablation selectively reduced EtOH drinking bouts. a–c Representative raster plots depicting individual licks (gray) and drinking bouts (blue) collected from control (top row) and FSI-ablated animals (bottom row) during the 2 h session across the 4-week DID paradigm. FSI ablation had no effect on the number of water drinking bouts (d) or sucrose drinking bouts (e). f Control animals escalated the number of EtOH drinking bouts during the 4-week DID paradigm, exhibiting a significant increase in weeks 3 and 4 versus week 1, while FSI-ablated animals exhibited significantly fewer EtOH drinking bouts compared to controls from weeks 2–4. FSI ablation had no effect on unorganized licking from animals drinking water (g), sucrose (h), or ethanol (i). * $p < 0.05$, ** $p < 0.01$. Data represented as mean \pm SEM.

Striatal FSIs may encode learning-dependent changes in action sequence expression [40, 41]. In addition, compulsive drinking rats adjust their lick frequency within drinking bouts [31]. Therefore, we next assessed lick frequency within drinking bouts across time (Fig. 4m–r). To do this, we categorized bouts into <3 Hz, 3–4 Hz, and >4 Hz lick frequency ranges, and expressed the data as relative frequency. We observed no main effect of FSI ablation on water bout lick frequency (<3 Hz: $F_{(1,19)} = 0.02$, $p = 0.88$; 3–4 Hz: $F_{(1,19)} = 0.20$, $p = 0.66$; >4 Hz: $F_{(1,19)} = 0.14$, $p = 0.72$, two-way ANOVA, Fig. 5m, p) or sucrose bout lick frequency (<3 Hz: $F_{(1,18)} = 1.76$, $p = 0.20$; 3–4 Hz: $F_{(1,18)} = 0.42$, $p = 0.53$; >4 Hz: $F_{(1,18)} = 0.59$, $p = 0.45$, two-way ANOVA, Fig. 4n, q). Additionally, we saw no main effect of time on bout microstructure across the four-week paradigm in either water drinking animal groups (<3 Hz: $F_{(2,39)} = 0.54$, $p = 0.59$; 3–4 Hz: $F_{(2.3, 45.4)} = 0.45$, $p = 0.68$; >4 Hz: $F_{(2.5, 47.9)} = 0.36$, $p = 0.75$, two-way ANOVA, Fig. 4m, p) or sucrose drinking animals (<3 Hz: $F_{(2.4, 42.8)} = 0.90$, $p = 0.43$; 3–4 Hz: $F_{(1.8, 33.5)} = 1.59$, $p = 0.22$; >4 Hz: $F_{(2.1, 37.1)} = 1.30$, $p = 0.29$, two-way ANOVA, Fig. 4n, q). However, we found a time \times ablation interaction from the ethanol drinking animals in the <3 Hz lick frequency ($F_{(3,54)} = 3.83$, $p < 0.05$, $\eta^2 = 0.10$) and a main effect of FSI ablation ($F_{(1,18)} = 12.5$, $p < 0.01$, $\eta^2 = 0.20$, Fig. 4o). We additionally observed that control animals exhibited an increase in <3 Hz bout licks at week 4 compared to week 1 that was not observed in FSI-ablated animals (week 1 control = 5.32 ± 1.15 %, week 4 control = 9.97 ± 1.49 %, $p < 0.05$, Dunnett’s multiple

comparisons test, Fig. 4o). Further, we found no main effects in 3–4 Hz events ($F_{(1,18)} = 0.81$, $p = 0.38$, two-way ANOVA), but found a main effect of FSI-ablation in >4 Hz events (control = 64.63 ± 1.62 %, FSI ablation = 76.13 ± 1.08 %, $F_{(1,18)} = 5.96$, $p < 0.05$, $\eta^2 = 0.16$, two-way ANOVA, Fig. 4r).

Finally, we examined the effect of FSI ablation on the expression of compulsive ethanol consumption (Fig. 5). Following the addition of the adulterant quinine into their respective drinking solutions we found that both water ($F_{(2.5, 33.5)} = 56.93$, $p < 0.001$, $\eta^2 = 0.67$, two-way ANOVA, Dunnett’s multiple comparison test, Fig. 5b) and sucrose drinkers reduced consumption relative to baseline ($F_{(2.8, 49.5)} = 39.7$, $p < 0.001$, $\eta^2 = 0.67$, two-way ANOVA, Dunnett’s multiple comparison test, Fig. 5c), but observed no main effect of FSI ablation in either group (water: $F_{(1,18)} = 0.58$, $p = 0.45$; sucrose: $F_{(1,18)} = 0.57$, $p = 0.46$, two-way ANOVA). However, we found a main effect of FSI ablation in the ethanol drinking mice ($F_{(1,68)} = 20$, $p < 0.001$, $\eta^2 = 0.18$, two-way ANOVA), where control animals exhibited greater quinine consumption compared to FSI-ablated animals (Dunnett’s multiple comparisons, Fig. 5d). Additionally, we found a main effect of time ($F_{(3,68)} = 5.0$, $p < 0.01$, $\eta^2 = 0.14$, two-way ANOVA), and found that control animals failed to reduce ethanol consumption with the addition of quinine (Dunnett’s multiple comparisons, Fig. 5d).

We next analyzed bout behavior from ethanol drinking animals during the three-day quinine challenge to assess whether FSI ablation affected quinine-adulterated lick microstructure. We



found that control animals exhibited more ethanol drinking bouts (control = 9.93 ± 1.05 bouts, FSI ablation = 5.68 ± 0.81 bouts, $t_{(18)} = 0.3143$, $p < 0.01$, $\eta^2 = 0.37$ Student's t test, Fig. 5e) and more unorganized licks than FSI ablated animals (control = 20.8 ± 3.59 licks, FSI ablation = 10.17 ± 1.80 licks, $t_{(18)} = 2.65$, $p < 0.05$, $\eta^2 = 0.28$, Student's t test, Fig. 5f). We additionally found that

control mice exhibited a greater relative frequency of <3 Hz licks (control = $10.85 \pm 6.5\%$, FSI ablation = $5.01 \pm 3.6\%$, $t_{(18)} = 2.6$, $p < 0.05$, $\eta^2 = 0.27$, Student's t test). No differences were observed in bout length ($t_{(18)} = 0.5$, $p = 0.63$, Student's t test, Fig. 5g) relative frequency ($F_{(1,64)} = 0.08$, $p = 0.77$, Fig. 5h) or bout variance ($t_{(18)} = 0.21$, $p = 0.84$, Student's t test, Fig. 5i).

Fig. 4 **Striatal FSI ablation selectively disorganized EtOH drinking bout microstructure.** **a–c** Representative raster plot of a 30 min window from a 2 h EtOH drinking session depicting individual licks (gray) and drinking bouts (blue) from control (top row) and FSI-ablated animals (bottom row). Inserts: magnification of an individual drinking bout illustrating the difference in bout length between control and FSI-ablated animals. **d–f** Mean bout length from control and FSI-ablated animals across drinking condition. FSI ablation had no effect on water (**d**) or sucrose (**e**) bout length, but increased mean bout length from EtOH-drinking animals (**f**). **g–i** A frequency distribution of drinking bouts binned by number of licks across drinking condition. FSI ablation had no effect on water (**g**) or sucrose (**h**) bout length distribution. **i** Control animals exhibited a greater proportion of small drinking bouts (three to four licks), while FSI ablated animals exhibited a greater proportion of larger drinking bouts (≥ 9 licks). **j–l** Drinking bout length variance across drinking condition. FSI ablation had no effect on bout length variance from water (**j**) and sucrose (**k**) drinking animals. **l** FSI ablation resulted in greater variability in the length of ethanol drinking bouts compared to control animals. Relative lick frequency collected from bouts during the 4-week drinking paradigm was binned into <3 Hz, 3–4 Hz, and >4 Hz ranges. FSI ablation had no effect on any lick frequency in water (**m, p**) or sucrose (**n, q**) drinking animals. However, control EtOH drinking animals exhibited a time-dependent increase in <3 Hz frequency licks that reached significance comparing week 1 versus week 4, which was not observed in FSI-ablated animals (**o**). Additionally, FSI-ablated animals exhibited fewer <3 Hz frequency licks than control animals at weeks 2–4. **r** An increase in >4 Hz frequency licks was observed in FSI-ablated animals as compared to control animals at week 2. * $p < 0.05$, ** $p < 0.01$, *** $p < 0.005$. Data represented as mean \pm SEM.

Since FSI-ablated ethanol-drinking animals exhibited reduced BEC levels compared to intact controls, we examined if BEC levels correlated with compulsive consumption. To do this, we averaged the three-day quinine consumption data to create a compulsive consumption score used for subsequent correlation analysis. We found no correlation between BEC level and compulsive consumption score in either the control group ($R^2 = 0.096$, $p = 0.38$), or FSI ablated group ($R^2 = 0.10$, $p = 0.37$). Additionally, we found no correlation between amount of ethanol consumed during the last week of DID and compulsive consumption in either control animals ($R^2 = 0.17$, $p = 0.23$) or FSI ablated animals ($R^2 = 0.05$, $p = 0.96$, Fig. 5j). We found a trend in the correlation between the number of ethanol bouts exhibited during the 4-week DID and compulsive consumption score (control: $R^2 = 0.35$, $p = 0.07$). This trend was not present in FSI-ablated animals ($R^2 = 0.05$, $p = 0.54$, Fig. 5k). Additionally, we found that the degree of variance in bout length exhibited during the 4-week DID paradigm negatively correlated with compulsive consumption score in control animals ($R^2 = 0.45$, $p < 0.05$) but not in FSI ablated animals ($R^2 = 0.23$, $p = 0.16$, Fig. 5l).

DISCUSSION

We found that FSI ablation did not impact any index of water or sucrose consumption, but reduced voluntary ethanol consumption and disrupted organized ethanol drinking microstructure by reducing the number of ethanol drinking bouts and increasing the number of licks within a bout. Further, FSI ablation significantly attenuated compulsive ethanol consumption, despite having no effect on ethanol (unadulterated) preference. Collectively, these data causally implicate striatal FSIs in the pathophysiology of compulsive alcohol drinking.

Repeated training of sequentially executed motor actions, like lever pressing, results in the organization and expression of action sequences that are optimally-timed for reward acquisition [36, 37]. Consistent with this, we found that control mice adapted their lick behavior over the four-week DID paradigm by selectively increasing the expression of ethanol drinking bouts, but not unorganized licks, which coincided with higher ethanol intake. Supporting the findings that the dorsal striatum is engaged during action sequence behavior [38–41], selective ablation of striatal FSIs disallowed the increase in the number of ethanol bouts and prevented the increase in relative expression of low frequency (<3 Hz) bout licks exhibited by control mice. These data therefore highlight a role for FSIs in organizing action sequences.

How FSIs organize action sequences remains an open question. Providing some clues, extant data demonstrates that FSIs are active during action sequence behavior [38, 41], and encode kinematic properties of action [42, 43] as ensembles [43] that regulate the concerted activity of striatal MSNs [42, 44–48]. Here we found that animals with intact FSIs exhibited distinct bout sequences centered around four licks per bout, while FSI-ablated

animals exhibited greater variability in bout length and, at times, exhibited unconstrained bouts of 20 or more licks. These data suggest that FSIs contribute to a learning process for habitual action sequence constraint, which is mediated by the dorsolateral striatum [49].

Chronic ethanol exposure promotes habitual behavior [3–7]. In line with this evidence, we found that four weeks of DID produced compulsive ethanol consumption. FSI ablation abolished this compulsive ethanol consumption but also reduced overall ethanol consumption during the DID paradigm. It is possible that FSI-ablated animals were incapable of achieving a compulsive drinking phenotype simply due to not preferring ethanol or insufficient total ethanol exposure over the course of the DID paradigm. However, FSI ablation did not affect ethanol preference. In addition, the degree of compulsive consumption and the amount of ethanol consumed (total licks) were not significantly correlated. This might suggest that the reduction in ethanol consumption in FSI-ablated animals during the four-week DID paradigm may instead be due to the removal of the organized, compulsive drinking component from overall consumption. Supporting this, control and FSI-ablated mice began the DID paradigm drinking an equivalent amount, but, over time, FSI-ablated animals failed to increase the number of drinking bouts compared to control animals.

Finally, we found that two elements of drinking behavior corresponded with compulsive ethanol consumption. Supporting rat data [31], we found organized drinking, expressed as the number of drinking bouts an animal exhibited during the four-week DID paradigm, positively correlated with the compulsive drinking score, while the variance in number of licks within a bout negatively correlated with the compulsive drinking score. During the quinine-adulterated ethanol challenge, FSI-ablated mice failed to exhibit compulsive drinking and this was met with a decrease in bout length. This contrasted with the FSI intact animals that displayed compulsive ethanol consumption and no such shift in bout length. Our interpretation is that FSI-ablated mice flexibly adapted their actions to curb compulsive drinking, while FSI-intact mice did not and, thus, persisted in drinking the quinine-adulterated ethanol. These data support previous work illustrating inflexible, organized lick microstructure in compulsive ethanol drinking rats [31] and identify a cellular substrate contributing to this effect.

Together, these data may suggest that alcohol targets FSIs to fuel the repeated execution of an organized action sequence, which ultimately leads to the compulsive behavior expression that is mediated, at least in part, by the dorsolateral striatum. Recent work reveals differential expression of G protein-coupled receptors in the putamen of alcohol use disorder patients and demonstrates that M4 muscarinic receptor activity regulates alcohol consumption in rats [50]. Whether alcohol regulates striatal FSIs through a mechanism mediated by the M4 muscarinic receptor requires future research. Given that the data herein support that elimination of less than 1% of all striatal neurons

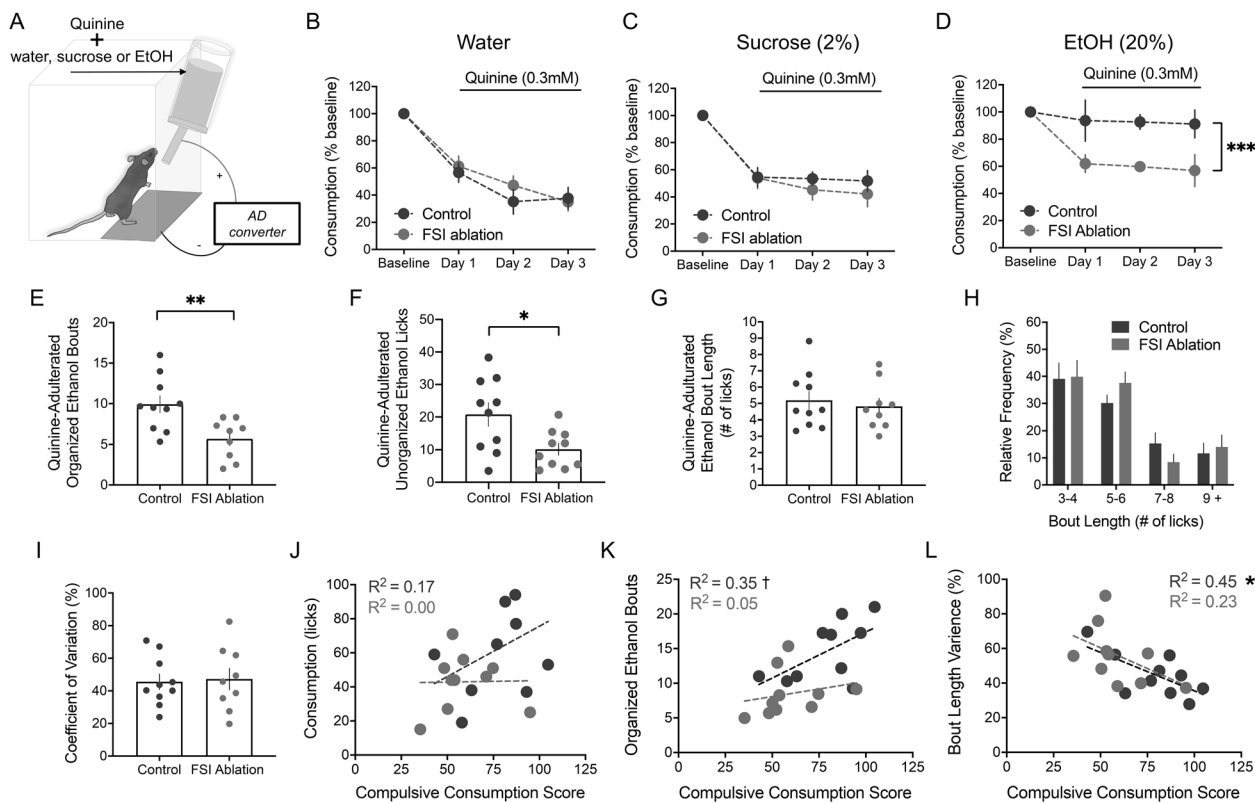


Fig. 5 Striatal FSI ablation attenuated compulsive EtOH consumption. **a** A schematic of the DID lickometer apparatus depicting for the quinine challenge that quinine is added to water, sucrose, or EtOH for water, sucrose, and EtOH drinkers, respectively, following the 4-week DID paradigm. **b–d** Fluid consumption from the three-day quinine challenge. With the addition of the bitterant quinine (0.3 mM), control and FSI-ablated animals exhibited reduced water (**b**) and sucrose consumption (**c**). **d** Control mice exhibited quinine-insensitive EtOH consumption, which was attenuated by FSI ablation across all three days. FSI ablation reduced the number of EtOH drinking bouts (**e**) and unorganized ethanol licks (**f**) during the quinine challenge. However, FSI ablation did not affect the mean bout length (**g**) or bout length distribution (**h**) or variance (**i**). **j** A correlation of the mean quantity of EtOH consumed during week 4 of DID with the degree of compulsive drinking during the 3-day quinine challenge. **k** A correlation of the mean number of EtOH drinking bouts during the 4-week DID paradigm with the degree of compulsive EtOH consumption in control and FSI ablated animals. **l** A correlation of EtOH drinking bout length variance from the 4-week DID paradigm with the degree of compulsive EtOH consumption. † $p = 0.07$, * $p < 0.05$, ** $p < 0.01$. Data represented as mean \pm SEM.

attenuates ethanol drinking and abrogates compulsive ethanol consumption, FSIs represent a compelling target for pharmacological intervention in alcohol use disorder.

FUNDING AND DISCLOSURE

This work was supported by The National Institute on Alcohol Abuse and Alcoholism grant R01AA024845 (B.N.M.). We report no financial interests or potential conflicts of interest.

AUTHOR CONTRIBUTIONS

M.S.P., C.K., and B.N.M. conceived experiments. M.S.P., M.H., C.K., and C.M. performed experiments. M.S.P. and B.N.M. wrote the manuscript with help from M.H., C.K., and C.M. B.N.M. secured funding.

ADDITIONAL INFORMATION

Publisher's note Springer Nature remains neutral with regard to jurisdictional claims in published maps and institutional affiliations.

REFERENCES

- Graybiel AM. Habits, rituals and the evaluative brain. *Annu Rev Neurosci*. 2005;31:359–87.
- Everitt BJ, Dickinson A, Robbins TW. The neuropsychological basis of addictive behaviour. *Brain Res Rev*. 2001;36:129–38.

- Sjoerds Z, Wit S, Brink W, Robbins TW, Beekman ATF, Pennix BWJH, et al. Behavioral and neuroimaging evidence for overreliance on habit learning in alcohol-dependent patients. *Transl Psychiatry*. 2013;3:1–8.
- Everitt BJ, Robbins TW. Drug addiction: updating actions to habits to compulsions ten years on. *Annu Rev Psychol*. 2016;67:23–50.
- Hopf FW, Chang SJ, Sparta DR, Bowers SM, Bonci A. Motivation for alcohol becomes resistant to quinine adulteration after 3 - 4 months of intermittent alcohol self-administration. *Alcohol Clin Exp Res*. 2010;34:1565–73.
- Lesscher HM, van Kerkhof LW, Vanderschuren JM. Inflexible and indifferent alcohol drinking in male mice. *Alcohol Clin Exp Res*. 2010;34:1219–25.
- Corbit LH, Nie H, Janak PH. habitual alcohol seeking: time course and the contribution of subregions of the dorsal striatum. *Biol Psychiatry*. 2012;72:389–95.
- Burch E, Makris N, Lee MR, Pallanti S, Hollander E. Compulsivity in alcohol use disorder and obsessive-compulsive disorder: implications for neuromodulation. *Front Behav Neurosci*. 2019;13:1–17.
- Garbusow M, Sebold M, Beck A, Heinz A. Too difficult to stop: mechanisms facilitating relapse in alcohol dependence. *Neuropsychobiology*. 2014;70:103–10.
- Kranzler HR, Soyka M. Diagnosis and pharmacotherapy of alcohol use disorder: a review. *JAMA*. 2018;320:815–24.
- Maisto SA, Hallgren KA, Roos CR, Witkiewitz K. Course of remission from and relapse to heavy drinking following outpatient treatment of alcohol use disorder. *Drug Alcohol Depend*. 2018;187:319–26.
- Stock AK. Barking up the wrong tree: why and how we may need to revise alcohol addiction therapy. *Front Psychol*. 2017;8:1–6.
- Ashby GF, Turner BO, Horvitz JC. Cortical and basal ganglia contributions to habit learning and automaticity. *Trends Cogn Sci*. 2010;14:208–15.
- Balleine BW, Delgado MR, Hikosaka O. The role of the dorsal striatum in reward and decision-making. *J Neurosci*. 2007;27:8161–5.
- Gremel CM, Costa RM. Orbitofrontal and striatal circuits dynamically encode the shift between goal-directed and habitual actions. *Nat Commun*. 2013;4:2264.

16. Knowlton BJ, Mangels JA, Squire LR. A neostriatal habit learning system in humans. *Science*. 1996;273:1399–402.
17. Yin HH, Mulcare SP, Hilário MR, Clouse E, Holloway T, Davis, et al. Dynamic reorganization of striatal circuits during the acquisition and consolidation of a skill. *Nat Neurosci*. 2009;12:333–41.
18. Dickinson A, Balleine B, Watt A, Gonzales F, Boakes RA. Motivational control after extended instrumental training. *Anim Learn Behav*. 1995;23:197–206.
19. Yin HH, Knowlton BJ, Balleine BW. Lesions of the dorsolateral striatum preserve outcome expectancy but disrupt habit formation in instrumental learning. *Eur J Neurosci*. 2004;19:181–9.
20. Yin HH, Knowlton BJ, Balleine BW. Blockade of NMDA receptors in the dorsomedial striatum prevent action-outcome learning in instrumental conditioning. *Eur J Neurosci*. 2005;22:505–12.
21. Yin HH, Knowlton BJ, Balleine BW. Inactivation of dorsolateral striatum enhances sensitivity to changes in the action-outcome contingency in instrumental conditioning. *Behavioural Brain Res*. 2006;166:189–96.
22. Gerfen CR, Surmeier DJ. Modulation of striatal projection systems by dopamine. *Annu Rev Neurosci*. 2011;34:441–66.
23. Kawaguchi Y. Physiological, morphological, and histochemical characterization of three classes of interneurons in the rat neostriatum. *J Neurosci*. 1993;13:4908–23.
24. Schlösser B, Bruggencate G, Sutor B. Local disinhibition of neocortical neuronal circuits causes augmentation of glutamatergic and GABAergic synaptic transmission in the rat neostriatum in vitro. *Exp Neurol*. 1999;157:180–93.
25. Luk KC, Sadikot AF. GABA promotes survival but not proliferation of parvalbumin-immunoreactive interneurons in rodent neostriatum: an in vivo study with stereology. *Neuroscience*. 2001;104:93–103.
26. Tepper JM, Koós T, Wilson CJ. GABAergic microcircuits in the neostriatum. *Trends Neurosci*. 2004;27:662–9.
27. Gittis AH, Nelson AB, Thwin MT, Palop JJ, Kreitzer AC. Distinct roles of GABAergic interneurons in the regulation of striatal output pathways. *J Neurosci*. 2010;30:2223–34.
28. O'Hare JK, Li H, Kim N, Gaidis E, Ade K, Beck J, et al. Striatal fast-spiking interneurons selectively modulate circuit output and are required for habitual behavior. *Elife*. 2017;6:e26231.
29. Blomeley CP, Cains S, Smith R, Bracci E. Ethanol affects striatal interneurons directly and projections neurons through a reduction in cholinergic tone. *Neuropsychopharmacology*. 2011;36:1033–46.
30. Patton MH, Roberts BM, Lovinger DM, Mathur BN. Ethanol disinhibits dorsolateral striatal medium spiny neurons through activation of a presynaptic delta opioid receptor. *Neuropsychopharmacology*. 2016;41:1831–40.
31. Darevsky D, Gill MT, Vitale KR, Hu B, Webner SA, Hopf FW. Drinking despite adversity: behavioral evidence for a head down and push strategy of conflict-resistant alcohol drinking in rats. *Addiction Biol*. 2018;24:426–37.
32. Tanahira C, Higo S, Watanabe K, Tomioka R, Ebihara S, Kaneko T, et al. Parvalbumin neurons in the forebrain as revealed by parvalbumin-cre transgenic mice. *Neurosci Res*. 2009;63:213–23.
33. Mathur BN, Tanahira C, Tamamaki N, Lovinger DM. Voltage drives diverse endocannabinoid signals to mediate striatal microcircuit-specific plasticity. *Nat Neurosci*. 2013;16:1275–85.
34. Rhodes JS, Best K, Belknap JK, Finn DA, Crabbe JC. Evaluation of a simple model of ethanol drinking to intoxication in C57BL/6J mice. *Physiol Behav*. 2005;84:53–63.
35. Wilcox MV, Carlson VC, Sherazee N, Sprow GM, Bock R, Thiele TE, et al. Repeated binge-like ethanol drinking alters ethanol drinking patterns and depresses striatal GABAergic transmission. *Neuropsychopharmacology*. 2014;39:579–94.
36. Botvineck MM, Yael N, Barto A. Hierarchically organized behavior and its neural foundation: a reinforcement-learning perspective. *Cognition*. 2009;113:262–80.
37. Dezfouli A, Lingawi NW, Balleine BW. Habits as action sequences: hierarchical action control and changes in outcome value. *Philos Trans R Soc B*. 2014;369:20130482.
38. Jin X, Costa RM. Start/stop signals emerge in nigrostriatal circuits during sequence learning. *Nature*. 2010;466:457–62.
39. Jin X, Tecuapetla F, Costa RM. basal ganglia subcircuits distinctively encode the parsing and concatenation of action sequences. *Nat Neurosci*. 2014;17:423–30.
40. Aldridge JW, Berridge KC. Coding of serial order by neostriatal neurons: a natural action approach to movement sequence. *J Neurosci*. 1998;18:2777–87.
41. Martiros N, Burgess AA, Graybiel AM. Inversely active striatal projection neurons and interneurons selectively delimit useful behavioral sequences. *Curr Biol*. 2018;28:560–73.
42. Kim N, Li HE, Hughes RN, Watson GDR, Gallegos D, West AE, et al. A striatal interneuron circuit for continuous target pursuit. *Nat Commun*. 2019;10:2715.
43. Roberts BM, White MG, Patton MH, Chen R, Mathur BN. Ensemble encoding of action speed by striatal fast-spiking interneurons. *Brian Struct Funct*. 2019;224:2567–76.
44. Bakhurin KI, Mac V, Golshani P, Masmanidis SC. Temporal correlations among functionally specialized striatal neural ensembles in reward-conditioned mice. *J Neurophysiol*. 2016;115:1521–32.
45. Duhne M, Lara-González E, Laville A, Padilla-Orozco M, Avila-Cascajares F, Arias-García M, et al. Activation of parvalbumin-expressing neurons reconfigures neuronal ensembles in murine striatal microcircuits. *Eur J Neurosci*. 2020. <https://doi.org/10.1111/ejn.14670>.
46. Gritton HJ, Howe WM, Romano MF, DiFeliceantonio AG, Kramer MA, Sligrama V, et al. Unique contributions of parvalbumin and cholinergic interneurons organizing striatal networks during movement. *Nat Neurosci*. 2019;22:586–97.
47. Klaus A, Planert H, Hjorth JJ, Berke JD, Silberg G, Kotaleski JH. Striatal fast-spiking interneurons: from firing patterns to post synaptic impact. *Front Syst Neurosci*. 2011;5:1–17.
48. Owen SF, Berke JD, Kreitzer AC. Fast-spiking interneurons supply feedforward control of bursting, calcium, and plasticity for efficient learning. *Cell*. 2018;172:683–95.
49. Rueda-Orozco PE, Robbe D. The striatum multiplexes contextual and kinematic information to constrain motor habits execution. *Nat Neurosci*. 2015;18:453–60.
50. Walker LC, Berizzi AE, Chen NA, Patricia R, Perreau V, Huckstep K, et al. Acetylcholine muscarinic M4 receptors as a therapeutic target for alcohol use disorder: converging evidence from humans and rodents. *Biol Psychiatry*. 2020; S0006-3223(20)30131–1.